

# Competitive Nucleation and Growth of $\{111\}$ $\Omega$ with $\{001\}$ GP Zones and $\theta'$ in a Stress-Aged Al-Cu-Mg-Ag Alloy

Shinji Muraishi\*, Shinji Kumai and Akikazu Sato

Department of Materials Science and Engineering, Tokyo Institute of Technology, Yokohama 226-8502, Japan

The stress aging method was conducted for an Al-Cu-Mg-Ag polycrystalline alloy to study the competitive nucleation and growth behavior of GP zones,  $\theta'$  and  $\Omega$  precipitates concurrently existing on different  $\{001\}$  and  $\{111\}$  habit planes. After initial stress aging for 1 h, the preferential nucleation of GP zones against  $\Omega$  occurred irrespective of the stress direction applied to the grains. With increasing aging time, the density of  $\Omega$  increased while the GP zones decreased in number to dissolve into the matrix, resulting from competitive nucleation due to the mutual constituent of Cu in GP zones and  $\Omega$ . With further stress aging, the growth of  $\theta'$  plates was enhanced in comparison with the growth of  $\Omega$  plates. The relative number density change between  $\{001\}$  and  $\{111\}$  precipitates was emphasized especially in grains with the stress direction along  $[001]$ , which indicated that nucleation and growth of GP zones and  $\theta'$  plates were highly sensitive to external stress compared with that of  $\Omega$ . HREM observation found that low amounts of small  $\Omega$  plates were nucleated during the initial stress aging indicating retarded  $\Omega$  nucleation. Two-step aging (stress aging for 1 h followed by the stress-free aging) revealed that preferentially nucleated GP zone against  $\Omega$  during the initial stress aging determined the successive precipitation sequence of the precipitation of  $\Omega$  and  $\theta'$ .

(Received May 6, 2004; Accepted August 23, 2004)

**Keywords:** aluminum copper alloy, transmission electron microscopy,  $\Omega$ , Guinier Preston zones,  $\theta'$ , stress aging

## 1. Introduction

Al-Cu alloys have been widely used for structural materials because of their good age hardening nature and high temperature creep resistance with the precipitation of GP zones and  $\theta'$  plates on  $\{001\}$  planes. Additional trace elements of Mg and Ag have been found to induce the finely dispersed  $\Omega$  precipitate on  $\{111\}_{\text{Al}}$  planes, replacing the conventional GP zones and  $\theta'$  plates on  $\{001\}_{\text{Al}}$  planes.<sup>1)</sup> This trace element effect on the precipitation of  $\Omega$  has been shown by atom probe field ion microscopy (APFIM) study<sup>2)</sup> as Mg-Ag clusters formed at the beginning of ageing, then Cu atoms aggregated into the clusters to form  $\Omega$  nuclei on  $\{111\}$  planes. Considering strain energy, Suh *et al.* have pointed out that the incorporation of Mg and Ag decreases the strain energy for the nucleation of  $\Omega$  on  $\{111\}$  plane.<sup>3)</sup> Since the  $\Omega$  precipitate exhibits basically the stoichiometric composition ratio of  $\text{Al}_2\text{Cu}$  compound and consequently changes into the stable  $\theta$  phase, the evolution of  $\Omega$  and  $\theta'$  precipitates should be closely related with the mutual constituent Cu atoms in GP zones,  $\theta'$  and  $\Omega$ . Previously we have reported the preferential nucleation of  $\Omega$  plates under external stress, nevertheless, stress effects on the nucleation and growth of GP zones and  $\theta'$ , which concurrently exists with  $\Omega$ , have been uncertain.<sup>4)</sup> The stress effect for GP zones has been examined by Eto.<sup>5)</sup> The continuous growth of GP zones into  $\theta'$  plate on  $\{001\}$  planes have been revealed by preparing the oriented GP zones in the stress aged Al-Cu alloy. Since the  $\Omega$  and also GP zones exhibit negative large misfit against the Al matrix, the different stress sensitivities of  $\Omega$  and GP zones causes the change of relative nucleation rates between  $\Omega$  and GP zones under stress, to determine the subsequent relative volume fraction and number density between  $\Omega$  and  $\theta'$ . In this work, stress aging has been performed to investigate the competi-

itive nucleation and growth behavior of  $\Omega$ , GP zones and  $\theta'$  plates on  $\{001\}$  and  $\{111\}$  planes in an Al-Cu-Mg-Ag polycrystalline alloy. The relative density change between  $\{001\}$  and  $\{111\}$  precipitates depending on the respective stress sensitivities of  $\Omega$ , GP zones and  $\theta'$  for the nucleation and growth have been investigated by observing the number density and average diameter change of  $\Omega$ , GP zones and  $\theta'$ . The stress effect on the nucleation period has been observed by HREM. The two-stepped ageing method (the combination of the stress and the stress-free aging) has been performed to study the effectiveness of the stress for the nucleation and growth periods.

## 2. Experimental Procedures

The chemical composition of the alloy was Al-6.3Cu-0.3Mg-0.5Ag (mass%). A cast slab of thickness 40 mm was homogenized at 743 K for 8 h in air, and hot-rolled down to a plate of 15 mm thickness. Average grain diameter was  $\sim 100 \mu\text{m}$ . Rectangular bar specimens ( $2 \times 2 \times 4 \text{ mm}^3$ ) were machined from the plate and used for the compressive stress-aging test. The external stress was applied on the specimen along the longest axis, which corresponded to the rolling direction. All specimens were solution heat treated for 1 h at 793 K and immediately quenched into iced water. Subsequently they were aged under compressive stress of 150 MPa for 1~196 h. The stress free aging was also performed for 1~196 h at 450 K. The two-stepped ageing (initial stress aging of 1 h followed by stress free aging of 10 h) was performed to examine the stress effect on the nucleation and growth behavior. TEM samples  $2 \times 3 \text{ mm}^2$  were cut from the aged specimens and mechanically thinned down to  $200 \mu\text{m}$ . All the TEM samples were cut from the specimen so that the stress direction would be parallel to the foil surface. The twin-jet-polish treatment was performed in a solution of 10% perchloric acid and 90% methanol at 238 K with voltage 14 V. Final polish treatment was made in a solution of 33% nitric acid and 66% methanol. The TEM observation was

\*Present address: Department of Metallurgy and Ceramic Science, Tokyo Institute of Technology, Tokyo 153-8552, Japan.  
Corresponding author, E-mail: muraishi@mtl.titech.ac.jp

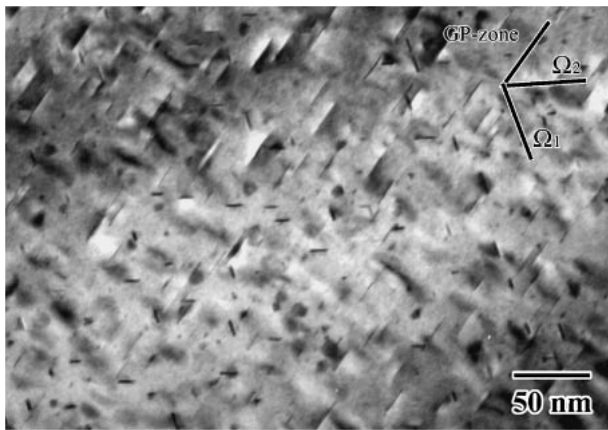


Fig. 1 TEM microstructure of the specimen aged for 0.16 h at 450 K. GP zones and  $\Omega$  phases were finely nucleated on  $\{001\}$  and  $\{111\}$  planes. Small dark spots dispersed were small  $\Omega$  nuclei.

done by JEM2011 (JEOL) and CM200 (Philips). In order to evaluate the stress effect of  $[001]$  and  $[111]$  directions independently, measurement of the number density and the diameter of precipitates was focused on the grains with stress directions along  $[001]$  and  $[111]$ . For the measurement of the number density, the observation was made where the TEM sample was 100 nm in thickness.

### 3. Experimental Results

#### 3.1 Stress effects on the precipitation microstructure of $\{111\}$ $\Omega$ , $\{001\}$ GP zones and $\theta'$

Typical microstructure of the aged specimen under the stress-free condition is shown in Fig. 1. The incident beam is along the  $[011]$  direction. In the figure, GP zones with diameter 20 nm are distributed on the  $\{001\}$  plane. Small  $\Omega$  plates with diameter 8 nm are dispersed on two of  $\{111\}$  planes, and the small dark spots observed in the image are small  $\Omega$  nuclei. In literature,<sup>6)</sup> it has been observed that the nucleation of  $\Omega$  phase occurred after 2 minutes at 450 K, followed by the nucleation of GP zones. Hence in this case, the nucleation of GP zones and  $\Omega$  plates occurred before 0.16 h. The precipitation of  $S'$  phase was not confirmed in the present work even after prolonged aging. Figure 2 shows the TEM microstructures of specimens aged at 450 K for 1 h under the stress-free condition (a); the compressive stress of 150 MPa with the direction along the  $[001]$  (b); and with the direction along  $[111]$  (c). The stress axis is shown in the figures. In Fig. 2(a),  $\Omega$  plates are dispersed on  $\{111\}$  planes together with GP zones on  $\{001\}$  planes, and the density of  $\Omega$  plate is almost the same as that of GP zones. The microstructures of stress-aged specimens with stress directions of  $[001]$  and  $[111]$  are shown in Figs. 2(b) and (c). Applying the stress significantly changes the relative density between GP zones and  $\Omega$  plates. In the case with the stress direction along  $[001]$  as shown in Fig. 2(b), the nucleation of GP zones is increased by the stress. Very little  $\Omega$  precipitate is observed in the image as compared with that of the stress-free aged specimen in Fig. 2(a), or with the specimen aged for 0.16 h in Fig. 1. The precipitation of  $\Omega$  plates is significantly suppressed by the additional stress with the stress direction of

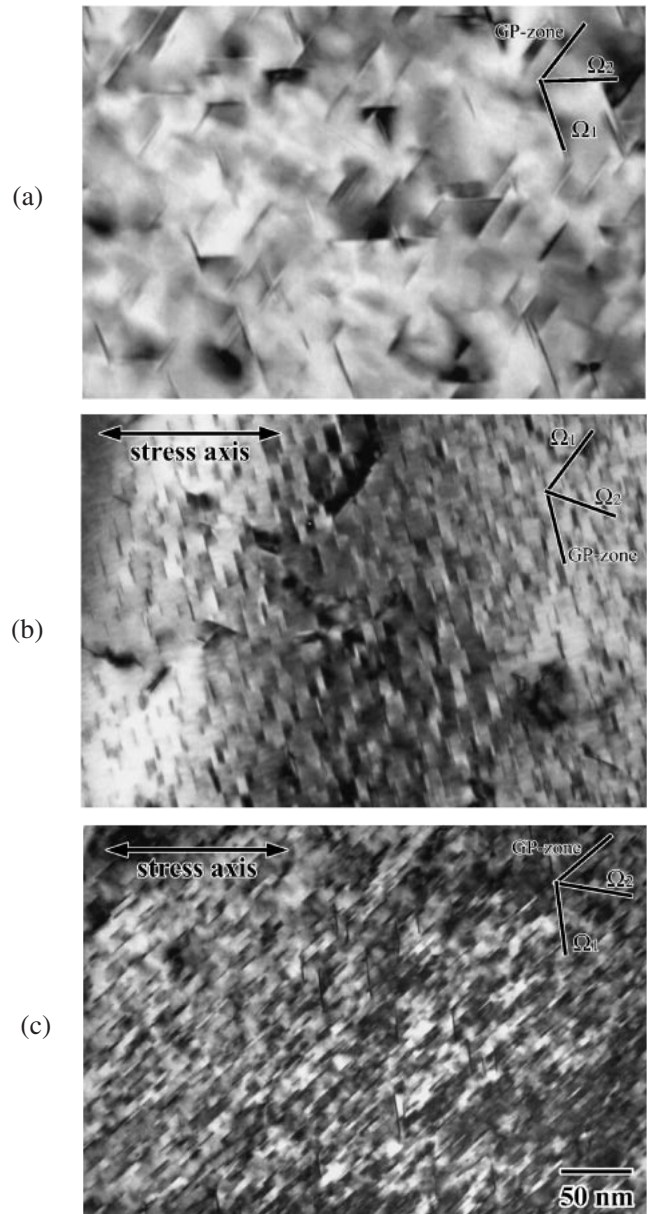


Fig. 2 TEM microstructure of the specimens aged at 450 K for 1 h. Stress-free condition (a), stress along  $[001]$  direction (b), and stress along  $[111]$  direction (c). Applied stress promotes the nucleation of GP zones irrespective to the stress direction, in contrast to the nucleation of  $\Omega$  plates.

$[001]$ . As for the grain where the promotion of  $\Omega$  precipitation would be expected with the stress direction along  $[111]$  in Fig. 2(c), applied stress exclusively promotes the nucleation of GP zones rather than that of  $\Omega$  plates. Considering that the promotion of GP zones occurs irrespective to the compressive stress direction as represented in Figs. 2(b) and (c), the nucleation of GP zones is highly sensitive to the external stress. The suppression of the nucleation of  $\Omega$  under the stress might be responsible for the promotion of GP zones.

TEM microstructures of the specimens aged for 196 h under the stress-free and the stress are shown in Fig. 3. Incident beam directions are  $\langle 011 \rangle$ . As shown in Fig. 3(a), the microstructure of the stress-free aged sample shows the finely dispersed  $\Omega$  precipitates on  $\{111\}$  planes to be the



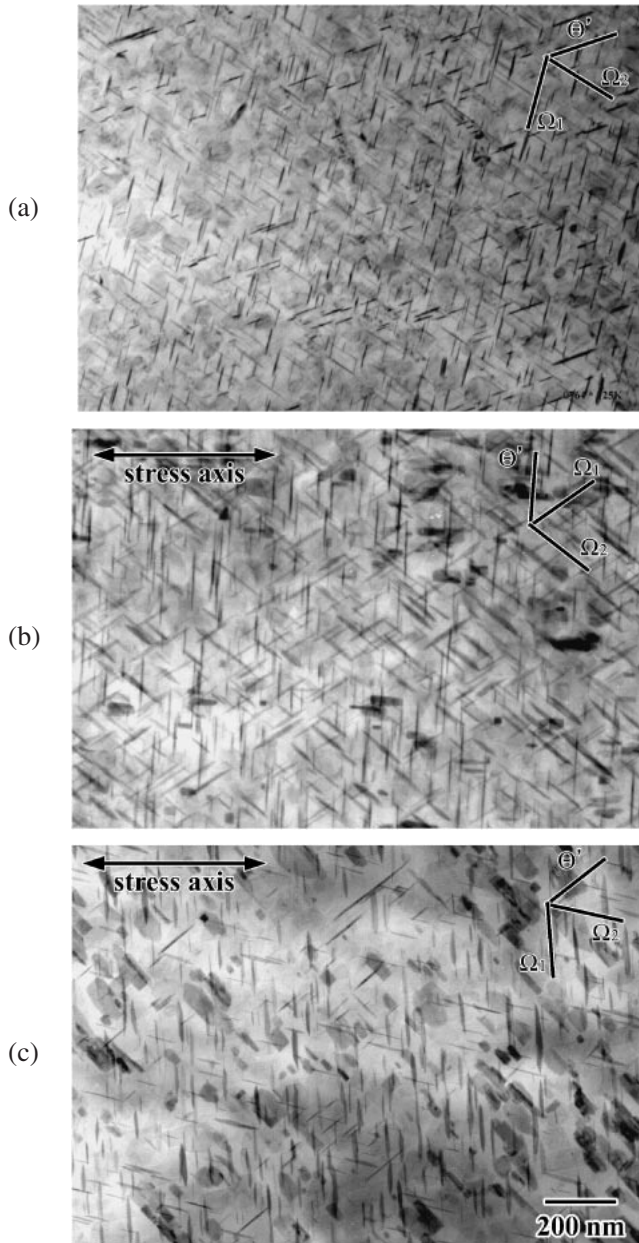


Fig. 3 TEM microstructure of the specimens aged at 450K for 196h. stress-free condition (a), stress along [001] direction (b), and stress along [111] (c). The external stress along [001] direction promotes the precipitation of  $\theta'$  variant perpendicular to the stress axis in (b). The external stress along [111] direction promotes the precipitation of the  $\Omega$  variant perpendicular to the stress axis in (c).

dominant phase. The precipitates observed on the (001) plane are  $\theta'$  plates which grew from GP zones. The total number density of  $\theta'$  plates are  $\sim 10\%$  of that of the  $\Omega$  plates in the stress-free condition. Figure 3(b) shows the microstructure of the specimen aged for 196h with the stress direction along [001]. The precipitation of  $\theta'$  plates is promoted by stress aging in comparison with the stress-free condition in Fig. 3(a). The growth of  $\theta'$  plate is apparently accelerated by the external stress, with the average size of  $\theta'$  plates at 80 nm for the stress-aged specimen and 50 nm for the stress-free aged specimen. The applied stress with the direction along [001] slightly affects the distribution of  $\Omega$  plates because of the equivalency of the [001] stress for {111}  $\Omega$

variants. The effect of the [111] stress direction on the aged microstructure is shown in Fig. 3(c). The stress-oriented  $\Omega$  plates are notably observed in the image, the density of  $\theta'$  plates is quite lower than that with the stress along [001] direction in (b). The relative density change of  $\theta'$  against  $\Omega$  depending on the stress direction suggests that the change of the relative nucleation and growth rates of  $\theta'$  against  $\Omega$ . Considering that the number density and diameter of  $\theta'$  plates are significantly changed by the additional stress, GP zones and  $\theta'$  are highly sensitive to the stress in the precipitation sequence in Al-Cu-Mg-Ag alloys.

### 3.2 Stress effects on the number density of {111} $\Omega$ , {001} GP zones and $\theta'$

#### 3.2.1 Definition of the number density of precipitates under the stress and stress-free conditions

The measurement of the number density of GP zones,  $\theta'$  and  $\Omega$  was carried out for the specimens aged for 0.16 to 196h. Figure 4 shows the change in the total number density of GP zones,  $\theta'$  and  $\Omega$  plate under the stress-free and the stress conditions as a function of aging time. The total number densities of GP zones,  $\theta'$  and  $\Omega$  plates are defined by the following way. The total number density ( $N_{\text{total}}$ ) of precipitates on three of {001} habit planes, GP zones or  $\theta'$  plates, is described as,

$$N_{\text{GP, total}} = N_{\theta', \text{ total}} = (N_A + N_B + N_C) \quad (1)$$

On the other hand,  $N_{\text{total}}$  of  $\Omega$  plates on four of {111} habit planes is described as,

$$N_{\Omega, \text{ total}} = (N_A + N_B + N_C + N_D) \quad (2)$$

Where,  $N_A$ ,  $N_B$ ,  $N_C$  and  $N_D$  are the number densities of the respective equivalent variant.

In the case of the stress-free condition,  $N_{\text{GP, total}}$  can be estimated from the number density accounting for the one variant ( $N_A$ ).

$$N_{\text{GP, total}} = 3N_A \quad (3)$$

In the same way,  $N_{\Omega, \text{ total}}$  is estimated as,

$$N_{\Omega, \text{ total}} = 4N_A \quad (4)$$

For the specimen aged under stress, the total number density is counted from typical grains with the stress direction along [001] and [111]. For example, as for the specimen with the stress along [001] direction,  $N_{\text{GP, total}}$  can be describes by using the number density of the one (001) variant, where the precipitation is promoted by the stress along [001] direction ( $N_{\text{promoted}}$ ).

$$N_{\text{GP, total}} = N_{\text{promoted}} \quad (5)$$

As for  $\Omega$ , the total number density of  $\Omega$  can be calculated from eq. (4), assuming that every {111}  $\Omega$  variant is equivalent to the stress direction of [001].

In the case with the stress along [111] direction,  $N_{\text{GP, total}}$  is calculated by using eq. (3), because all the three {001} variants are equivalent to the stress along [111] direction. From the experimental data of stress-oriented  $\Omega$  plates,<sup>4)</sup> the number density of stress-promoted  $\Omega$  variant ( $N_{\text{promoted}}$ ) was found to be twice that of the other suppressed  $\Omega$  variant ( $N_{\text{suppressed}}$ ). Namely,  $N_{\text{suppressed}} = 1/2 N_{\text{promoted}}$ .  $N_{\Omega, \text{ total}}$  is

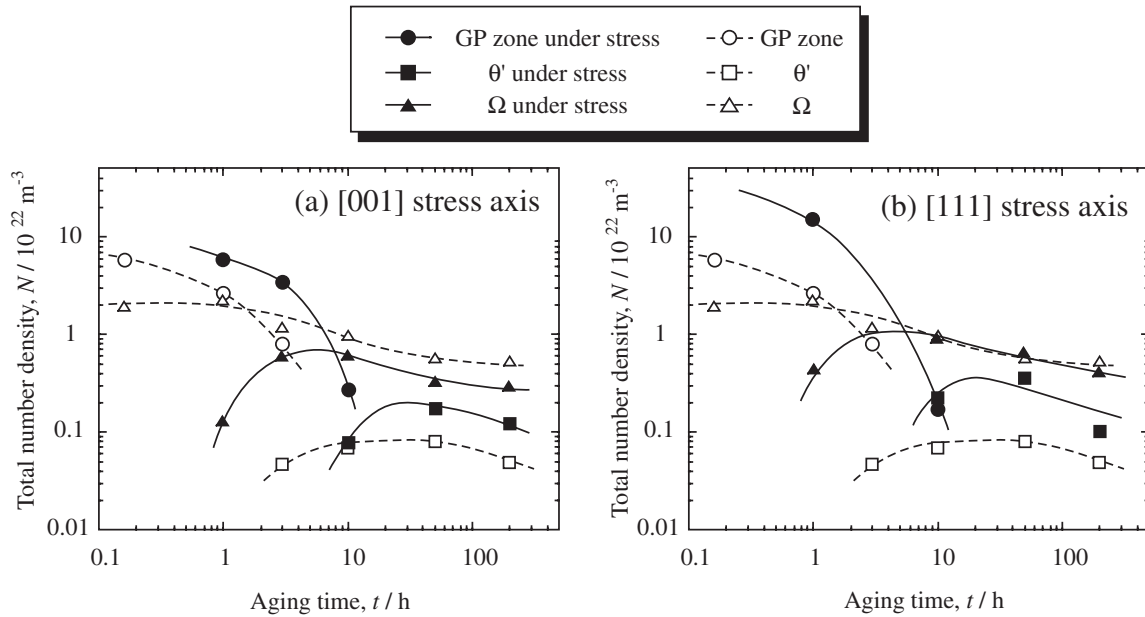


Fig. 4 The number density change against the aging time. Stress-free (a); and stress along [001] and [111] directions (b). The nucleation of GP zones is highly promoted at initial stage of stress aging.

consequently described as,

$$N_{\Omega, \text{ total}} = (N_{\text{promoted}} + 3N_{\text{suppressed}}) = 2.5N_{\text{promoted}} \quad (6)$$

### 3.2.2 Effects of the [001] compressive stress on the number density of precipitates

The number densities of GP zones,  $\theta'$  and  $\Omega$  were counted for the aged specimens and the effect of the stress direction of [001] is shown in Fig. 4(a). The number densities of precipitates under the stress-free condition are also plotted as reference. At the initial stage of aging, at 0.16 h, the number densities of  $\Omega$  and GP zones under the stress free condition are  $2 \times 10^{22}$  and  $6 \times 10^{22} \text{ m}^{-3}$ , respectively. The values for GP zones are initially higher than that of  $\Omega$ , and with increasing aging time, a gradual increase of  $\Omega$  density is observed in contrast with the rapid decrease in the density of GP zones. The  $\theta'$  plates are observed after 3 h with their final density reaching 10% of  $\Omega$  plates.

Compressive stress changes the relative density of {001} against {111} precipitates and generally increases the density of GP zones and  $\theta'$  on {001} habit planes. After 1 h of stress aging, low amounts numbers of  $\Omega$  plates are detected within the grain with density at  $0.1 \times 10^{22} \text{ m}^{-3}$ . The dominant GP zones are measured at  $6 \times 10^{22} \text{ m}^{-3}$ . However, the density of GP zones rapidly decreases to  $0.2 \times 10^{22} \text{ m}^{-3}$  after 10 h. The density of  $\Omega$  increases to  $0.6 \times 10^{22} \text{ m}^{-3}$  after 3 h, after which it gradually decreases. This indicated that the additional stress firstly assists the formation of GP zones, after which the nucleation of  $\Omega$  simultaneously occurs with the dissolution of GP zones into the matrix.  $\theta'$  plates are observed after 10 h of stress aging. The density of  $\theta'$  phase is  $0.2 \times 10^{22} \text{ m}^{-3}$  at 50 h, which is 2.3 times larger than that of the stress-free condition at the same aging time. Increments of the  $\theta'$  density corresponding to decrements of the  $\Omega$  density is observed in the figure. After further aging, the relative densities of  $\theta'$  and  $\Omega$  remains almost constant. Excessively nucleated GP zones at the initial stage of aging

seems to control the following nucleation and growth of  $\theta'$  and  $\Omega$  plates.

### 3.2.3 Effects of the [111] compressive stress on the number density of precipitates

The effect of the [111] stress direction on the number density change is shown in Fig. 4(b). Stress in the [111] direction during initial aging promotes the nucleation of GP zones rather than that of  $\Omega$ , as observed also in the specimen with the stress direction of [001] in Fig. 4(a). The increase in GP zone density irrespective of the stress directions at the initial stage of aging in Figs. 4(a) and (b) shows that GP zones are highly sensitive to external stress. After 10 h of stress aging, the numbers of  $\Omega$  reach a similar density to that of the stress-free condition. Since the increase in  $\theta'$  density is simultaneously observed with the increase in  $\Omega$  density, the nucleation of  $\theta'$  is apparently promoted under the stressed condition.

## 3.3 Stress effects on the average diameter of {111} $\Omega$ , {001} GP zones and $\theta'$

### 3.3.1 Effect of the [001] compressive stress on the average diameter of precipitates

The average diameters of  $\Omega$ , GP zones and  $\theta'$  were measured for specimens aged for 0.16~196 h at 450 K under the stress and the stress-free conditions. Figure 5 shows the average diameter of  $\Omega$ , GP zones and  $\theta'$  as a function of aging time. Since GP zones and  $\theta'$  concurrently exists on {001} variants, precipitates with diameters under 30 nm were regarded as GP zones. The diameter of GP zones under the stress-free condition are 20 nm after 3 h of aging. After that, GP zones change into  $\theta'$  with diameter 30 nm at 10 h. The diameter of  $\theta'$  gradually increases to 55 nm at 196 h. Rapid growth of  $\Omega$  is observed from 8 nm at 0.16 h and 50 nm at 10 h. At 196 h, the diameter of  $\Omega$  is 65 nm. The rapid growth of  $\Omega$  up to 10 h indicates that the  $\Omega$  phase replaces GP zones as the dominant phase. This dominant formation of  $\Omega$

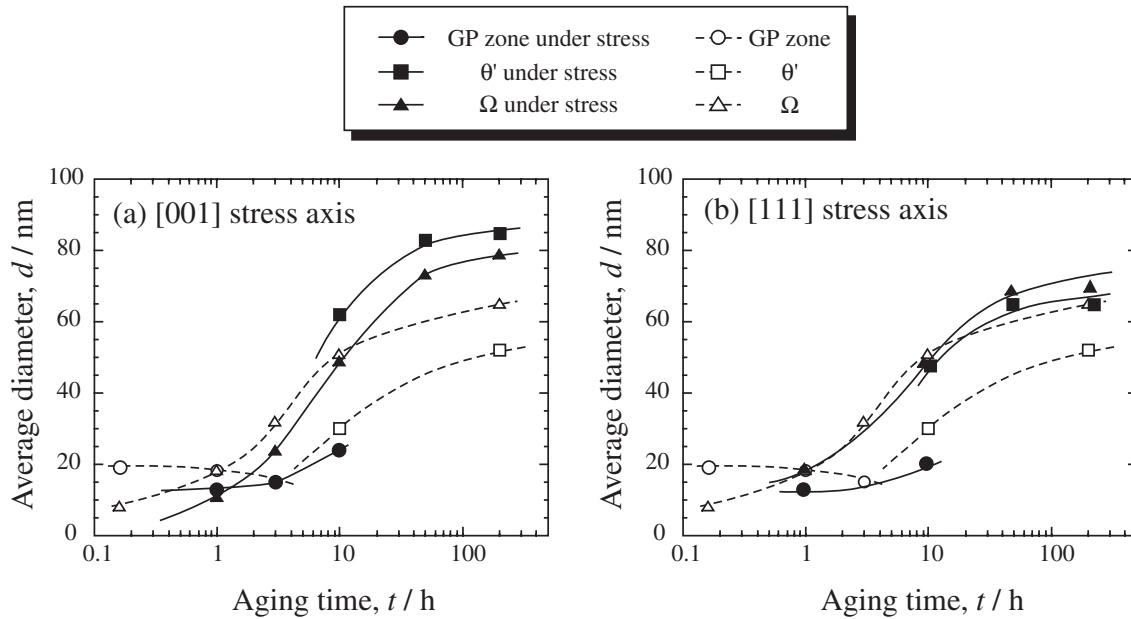


Fig. 5 Average diameter change against aging time under stress-free and stress along [001] direction (a) and [111] direction (b). The growth of  $\theta'$  plates is emphasized by stress along the [001] direction.

suggests that most of the GP zones dissolve into the matrix to form  $\Omega$  while the rest continuously grow to  $\theta'$ .

The lower GP zone diameter in comparison to the stress free case indicates that the external stress yields fine nucleation of GP zones with a large number density. Also, the  $\theta'$  diameter rapidly increases to 62 nm after 10 h and 85 nm at 196 h. As compared with the stress free condition, the growth of  $\theta'$  is significantly accelerated by stress aging. The  $\Omega$  diameter is less than that under the stress-free condition up to 10 h, which is attributed to fine nucleation. After 10 h, the  $\Omega$  diameter is larger than that under the stress free condition, with the growth of  $\Omega$  plates accelerated by external stress.

### 3.3.2 Effect of the [111] compressive stress on the average diameter of precipitates

The average diameters of precipitates aged under the stress-free and stress along [111] direction are shown as a function of aging time in Fig. 5(b). GP zones exhibit small diameters of 13 nm at 1 h, which is comparable to that of the [001] stress condition. Accounting for the promotion of GP zone density in Fig. 4(b), fine nucleation of GP zones occurs under stress along the [111] direction as well as that under stress along the [001] direction.  $\theta'$  plates exhibit larger diameters than that under the stress-free condition, of 48 nm at 10 h and 64 nm at 196 h. As compared with the diameter change under the stress along [001] direction in Fig. 5(a), the growth of  $\theta'$  plates are more sensitive to the stress direction of [001] than that of [111]. The tendency of the diameter change of  $\Omega$  is almost identical between the stress along [111] direction and [001] directions, with the external stress inducing the fine nucleation and the accelerated growth. As a consequence, the diameters of GP zones and  $\Omega$  at the initial stage of stress aging are less than that under the stress-free condition. The diameter of  $\theta'$  is especially large in stress-aged specimens. Since large increments of the number densities due to external stress are observed for GP zones and  $\theta'$  in

Figs. 4(a) and (b), precipitation density on {001} planes is significantly promoted under compressive stress.

## 4. Discussion

### 4.1 HREM observation of the early stage of $\Omega$ plates

The application of external stress causes the promotion of GP zones and the retardation of  $\Omega$  during the initial stage of aging. The results of the number densities and diameter changes due to stress in Figs. 4 and 5, suggest that changes in the nucleation rates yield different precipitation densities on the {001} and {111} planes. In order to examine the small  $\Omega$  density under external stress, HREM observation was conducted for  $\Omega$  precipitate at the early stage of stress aging. Figure 6 shows the HREM image of the specimen aged for 1 h with compressive stress of 150 MPa. The slight contrast of  $\Omega$  is observed in the strong strain contrast caused by GP zones. It should be mentioned that  $\Omega$  plate is hardly observed in comparison to GP zones. From literature,<sup>1)</sup>  $\Omega$  phase has an orthorhombic structure with the  $c$  axis corresponding to the four {111} Al planes. The  $\Omega$  observed in Fig. 6 consists of two {111} Al planes corresponding to the 1/2 of the  $c$  axis of  $\Omega$  unit cell. Since similarly thin  $\Omega$  with fairly weak contrast has been reported in the initial stage of aging,<sup>7)</sup> the small  $\Omega$  with the 1/2 thickness might be the nuclei of  $\Omega$  plates. Noting that under stress, the  $\Omega$  phase scarcely nucleates at the beginning and finally becomes the dominant phase after further stress aging, the low density of  $\Omega$  at the initial stage is attributed to the high stress sensitivity of GP zone formation causing the shortage of Cu content required for the nucleation of  $\Omega$ . In addition, since the nucleation of  $\Omega$  plates naturally follows the formation of GP zones,<sup>2)</sup> the nucleation and growth of  $\Omega$  plates is further delayed due to the excessively nucleated GP zones under the external stress.



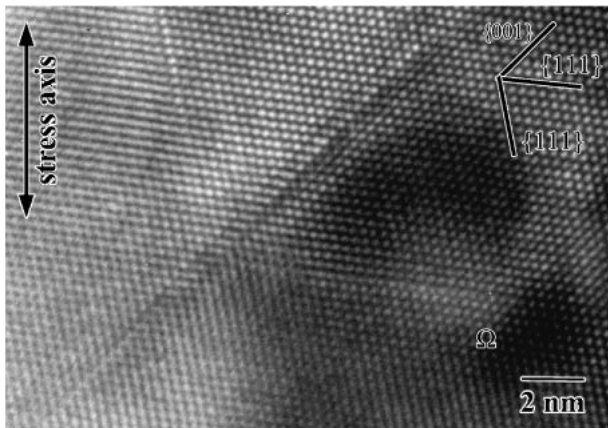


Fig. 6 HRTEM image of the specimen aged under the stress for 1 h. Faint contrast of  $\Omega$  phase is observed as marked among the dark strain contrast from GP zones.

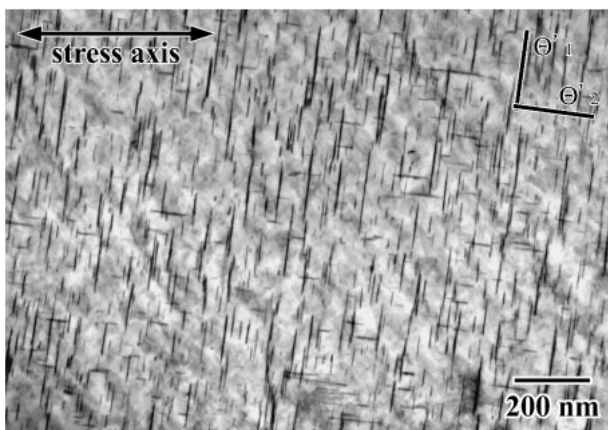


Fig. 7 Microstructure of the specimen aged under the stress for 3 h at 450 K followed by stress-free aging for 10 h at 450 K. Stress effect on the growth of  $\theta'$  plates is almost determined during the nucleation period.

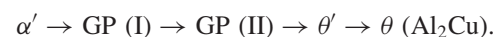
#### 4.2 The stress effect on the growth of $\theta'$

The present study found that the growth of  $\theta'$  plates is especially accelerated by additional stress. The rapid growth of  $\theta'$  under the stress condition suggests an increase in the relative volume fraction of  $\theta'$  against  $\Omega$  during the stress aging. In order to examine the stress effect on the growth of  $\theta'$  plates, two-step aging (the initial stress aging followed by the stress-free aging) was conducted. Figure 7 shows the microstructure of the specimen aged under the compressive stress for 3 h at 450 K, and then followed by the stress-free aging for 10 h at 450 K. Observation was carried out for the grain with the stress along  $[001]$  direction. Incident beam is along the  $[100]$  direction. The stress-orienting effect of  $\theta'$  is clearly observed in the figure. The degree of orienting was measured to be 0.6, which is not completion of oriented  $\theta'$  but almost comparable to that observed in stress oriented  $\theta'$  by Eto.<sup>5)</sup>  $\theta'$  plates perpendicular to the compressive stress are large in size and volume in comparison with the other variant parallel to the stress axis. The average diameter of  $\theta'$  plate is measured to be 64 nm, which exhibits almost the same value as that of the continuously stress-aged specimen for 10 h ( $\sim 60$  nm). The accelerated growth of  $\theta'$  observed by two-step

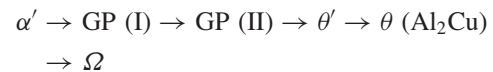
aging indicates that the distribution of  $\theta'$  phase is almost determined at the first step of stress aging. Since  $\theta'$  precipitation was not observed at 3 h of stress aging as shown in Fig. 4(a),  $\theta'$  represented in Fig. 7 develops from the stress-oriented GP zones introduced during the first step of stress aging. Hence, the accelerated growth of  $\theta'$  plates under stress results from the stress-assisted GP zones effectively working as the precursor phase to assist the following nucleation and growth of  $\theta'$  plates.

#### 4.3 The stress effect on the precipitation sequence of $\Omega$ phase and GP zones

The precipitation of GP zones and  $\theta'$  facilitates by the application of stress irrespective of the stress direction, and consequently delays the precipitation of  $\Omega$ . The sequence of  $\theta$  precipitation in an Al-Cu binary alloy system is as follows,



From literature,<sup>8)</sup> the nucleation of  $\Omega$  and GP zones in the Al-Cu-Mg-Ag alloy independently occurred at the initial stage of aging. The precipitation sequence is as follows,



Suh and Park<sup>3)</sup> reported that addition of Mg and Ag decreases the formation energy of disk shaped clusters on  $\{111\}$  planes. However since GP zones first formed then disappeared with increasing  $\Omega$  density, the higher nucleation rate of GP zones compared to that of  $\Omega$  is suggested to cause the preferred clustering of Cu atoms on  $\{001\}$  planes at initial stage of aging. Furthermore, the low density of  $\theta'$  (10% of total precipitates) indicates that the growth of  $\Omega$  on  $\{111\}$  habit planes is preferred rather than the continuous growth of GP zones into  $\theta'$  plate on  $\{001\}$  habit plane in the Al-Cu-Mg-Ag alloy system.

Taking into account the above precipitation sequence, the external stress facilitates the nucleation of GP zones by enhancing the nucleation rate of GP zones. In addition, assuming that the spherical Mg-Ag clusters exhibit small non-directional eigen strains,<sup>2)</sup> the stress assisted nucleation of  $\Omega$  is not be expected.

Hence, the difference in the relative precipitation density between  $\{001\}$  and  $\{111\}$  planes (Figs. 4 and 6) under applied stress is caused by the excessively nucleated GP zones, which suppress the nucleation of  $\Omega$  and promote the successive growth of  $\theta'$ .

#### 5. Conclusions

Effects of external stress on the nucleation and growth of  $\{111\}$   $\Omega$ ,  $\{001\}$  GP zones and  $\theta'$  precipitates were investigated in an Al-Cu-Mg-Ag polycrystalline alloy. Applying the stress during the aging, the external stress facilitates the formation of GP zones and  $\theta'$  on  $\{001\}$  planes. In contrast, a lower density of  $\Omega$  precipitation occurs under stress in comparison with that under the stress-free condition, especially for grains with stress direction along  $[001]$ . The dominant nucleation of GP zones during the initial stress aging results from high stress sensitivity and acts to retard the nucleation of  $\Omega$ . HREM observation for the initial stress aged

specimen showed the low amounts of dispersed  $\Omega$  nuclei, which indicated the delayed nucleation of  $\Omega$  against GP zones. The two-step aging revealed that external stress during initial aging induces the preferential nucleation of GP zones which assists the successive  $\theta'$  precipitation and consequently suppress the nucleation and growth of  $\Omega$ .

### Acknowledgements

The present authors would like to express the gratitude to M. Nakai and T. Eto at Kobe Steel Ltd. and Light Metal Educational Foundation Inc. for the alloy preparation and partial financial support.

### REFERENCES

- 1) B. C. Muddle and I. J. Polmear: *Acta Metall.* **37** (1989) 777–789.
- 2) M. Murayama and K. Hono: *Scr. Metall.* **38** (1998) 1315–1319.
- 3) I. S. Suh and J. K. Park: *Scr. Metall.* **33** (1995) 205–211.
- 4) S. Muraishi, S. Kumai and A. Sato: *Philos. Mag A* **82** (2002) 415–428.
- 5) T. Eto, A. Sato and T. Mori: *Acta Metall.* **26** (1978) 499–508.
- 6) L. Reich, M. Murayama and K. Hono: *Acta Mater.* **46** (1998) 6053–6060.
- 7) Q. Cui, G. Itoh and M. Kanno: *J. Japan Inst. Metals* **59** (1995) 492–501.
- 8) K. Hono, N. Sano, S. S. Babu, R. Okano and T. Sakurai: *Acta Metall.* **41** (1993) 829–838.